THE JOURNAL OF PHYSICAL CHEMISTRY B

ARTICLE

pubs.acs.org/JPCB

Critical Effects on Attractive Solutes in Binary Liquid Mixtures Close to Their Consolute Point: A New Experimental Strategy

Karin I. Gutkowski,[†] Roberto Fernández-Prini,[†,‡] Pedro F. Aramendía,[‡] and M. Laura Japas*[,†,§]

[†]Gerencia Química, CAC, Comisión Nacional de Energía Atómica, Avenida Libertador 8250, 1429-Buenos Aires, Argentina

[‡]INQUIMAE/DQIAQF, Facultad de Ciencias Exactas y Naturales, Universidad de Buenos Aires, Ciudad Universitaria, Pabellón II, 1428-Buenos Aires, Argentina

[§]Escuela de Ciencia y Tecnología, Universidad Nacional de San Martín, Martín de Irigoyen 3100, 1650-San Martín, Provincia Buenos Aires, Argentina

ABSTRACT: The effect of near-criticality upon the properties of dilute solutions of attractive solutes has been previously studied only using pure solvents close to the vapor−liquid critical point. The experimental difficulties that plague this thermodynamic region have somewhat obscured the interpretations of the results. Consequently, the coupling of long-range critical fluctuations with short-range intermolecular interactions is still a matter of debate. We developed a new strategy consisting of studying the changes in the solvation shell of probe molecules dissolved in a binary solvent mixture close to its lower consolute critical point. The study is based on UV−vis absorption and fluorescent emission measurements of the solvatochromic and thermochromic effects of two dyes, Reichardt's Dye and Nile Red, dissolved in mixtures of lutidine−water. The results show unambiguously the existence of a subtle change in the composition of the near-critical solvent surrounding the probe molecules with respect to the bulk composition, thus we conclude that the coupling of long-range fluctuations with short-range interactions is now firmly established.

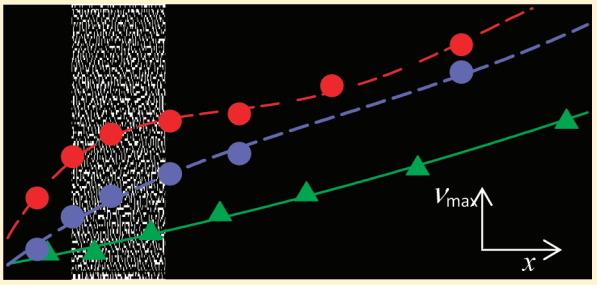

INTRODUCTION

Supercritical fluids (SCFs) have been thoroughly studied during the last decades as they exhibit peculiar physicochemical behavior and are being employed in several technological processes replacing conventional solvents.[1] The main physicochemical feature that makes SCFs interesting as solvents is their high compressibility; near their critical point, small variations in pressure (or temperature) have a very large effect in their density and therefore in their solvation power. As a consequence of its high mechanical susceptibility, the critical vicinity is signaled by large density fluctuations, these produce domains of liquid-like and gas-like densities whose size, given by the correlation length ξ, grows approaching the critical point. Then, regarding the role of SCFs as solvents, a relevant question is how solvation of solutes is affected at near-critical conditions by the long-range correlation between solvent molecules.

Several studies carried out in the last two decades showed that, near the solvent's critical point, the average *local* density of the solvent around an attractive solute is significantly larger than the average *bulk* density, a phenomenon denominated local density augmentation (LDA). Reported experimental values of local densities were up to 3 times larger than bulk densities.[2−5] In addition, a number of theoretical studies have been dedicated to search on LDA by means of integral equation approaches[3,6,7] or computer simulations.[8,9]

The increase in solvent density around an attractive solute molecule is an evidence of strong solute−solvent interactions, compared with those between solvent molecules, and can also be observed beyond critical conditions. However, in addition, when the solvent is near its critical point, the strong correlation between solvent molecules can couple to the direct intermolecular interactions and, indirectly, accentuate the inhomogeneity around the solute. The relative importance of these two effects on the LDA phenomena observed near critical conditions is a subject of debate.

For the case of simple solutes in pure solvents, the effect of solvent criticality on equilibrium and dynamic properties was investigated by measuring shifts in electronic absorption spectra,[10−12] or in the frequency of vibrational transitions,[13,14] fluorescence emission spectra,[15−17] fluorescence anisotropy,[18] free radical reaction,[19,20] Raman bandwidth,[21] and rotational[22] and vibrational relaxations.[23] Some of these studies indicate that, near the solvent's critical temperature, many properties show a plateau in their density dependence, i.e., there is a density range in which the properties of the solute are practically independent of solvent density. The size of this region, centered at densities smaller than the critical density, diminishes very strongly with the increase of the temperature from the gas−liquid critical point. These anomalies were assigned to a LDA of the solvent around the solute due to a coupling between the high mechanical

Received: September 17, 2011
Revised: November 4, 2011
Published: November 10, 2011

dx.doi.org/10.1021/jp209007y | *J. Phys. Chem. B* 2011, 115, 15303–15312

susceptibility of the solvent and the strong cross interactions. However, the inherent experimental difficulties in studying near-critical systems are an obstacle to establish, beyond doubt, the existence of criticality-induced density changes in the solvation shell of a probe molecule. Temperature inhomogeneities are the most common source of distortion, essentially because density is seldom measured but usually obtained from the determined values of the pressure and temperature by using an equation of state (EoS) for the pure solvent. However, due to the divergence of the compressibility, experimental errors in p and T propagate in the calculation of the density with unusual amplification, which can lead to erroneous conclusions. As an example, Urdahl et al.[13] reported anomalies (existence of a plateau) in the vibrational shifts and lifetimes of $W(CO)_6$ in supercritical ethane. However, after repeating the measurements with a more accurate determination of the pressure and a careful elimination of temperature gradients, a normal dependence was found.[24]

Moreover, in almost all the experimental studies, the density of the quasi-critical solvent is calculated assuming the presence of the solute does not affect the relation between the state variables p, ρ, and T. The essential problem is that, at the solvent's critical point, besides $(\partial V/\partial p)_T$ and $(\partial V/\partial T)_p$, also $(\partial V/\partial x)_{T,p}$ diverges, and therefore a non-negligible concentration of the solute can introduce considerable uncertainty in the bulk density values.[25] For these reasons, we consider that the question of the effects of critical fluctuations on solvation does not yet have a conclusive answer.

In this context, and in order to avoid experimental flaws, a possible alternative is to study systems with similar characteristics but such that they allow an improvement in the precision of the measurements. Partially miscible binary systems with liquid−liquid (consolute) critical points near room temperature at atmospheric pressure are good candidates. As 1-component liquid−vapor critical points, systems near liquid−liquid critical points exhibit large susceptibility (osmotic, instead of mechanical) and the concomitant existence of fluctuating domains, characterized by the difference in their mole fraction x. Therefore, according to the principle of universality of critical phenomena,[26] if LDA has a critical-phenomenon origin, the *local composition* around a solute molecule should be affected in the neighborhood of a liquid−liquid critical point.

Solute molecules dissolved in binary solvent solutions generally show a solvation shell whose composition differs from the bulk concentration. The phenomenon is known as *preferential solvation*, and it exists over all the thermodynamic one-phase space, i.e. even far from critical conditions. Here the relevant question is whether the local composition around a probe molecule is altered as the critical point is approached.

There are two essential advantages of studying consolute points: first, the experimental simplicity and precision since there are several systems with liquid−liquid critical points near room temperature and atmospheric pressure. In this regard, experimental studies of systems near liquid−liquid critical points have played a paramount role in understanding Coulombic criticality,[27] whereas the information gathered from studies of vapor−liquid critical points lacked the required precision.[28] More important, the second advantage is that the variable showing strong fluctuations (the order parameter) near a consolute point is the solvent's *composition*, a magnitude of easy experimental control as compared with the density of the fluid, and one that is directly determined instead of inferred by an EoS. This is an important difference, as in our opinion the weakest aspect of most experimental LDA studies in SCFs is not the characterization of the local density around a probe but its proper assignment to a solvent's bulk density.

Scheme 1. Structure of RD (a) and NR (b)

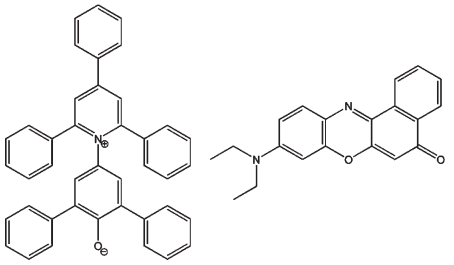

(a) (b)

Optical probes have been extensively used to monitor the molecular environment, since the early works of Mc Rae[29] and Lippert and Mataga.[30] Absorption or emission spectroscopy is mostly used because of the ease of measurement. Solvatochromism is the effect that induces shifts in the energy of the absorption or the emission due to changes in the overall interaction between the environment and the probe.[31−33] These changes are enhanced when the two electronic states involved in the transition have very different features. Changes in polarity are particularly effective, but the overall solvation ability, including changes in specific and nonspecific interactions of probe electronic states and environment, are the actual cause of spectral shifts. Emission studies, having lower detection limit and thus requiring lower probe concentration, are influenced by dynamic as well as equilibrium phenomena.[34]

In absorption spectroscopy, solvatochromic effects take into account the difference in energy between the equilibrated ground state and the Franck−Condon configuration of the electronically excited state. Instead, the emission process is more complex: the relaxation within the excited state electronic surface—from the initially excited Franck−Condon configuration to the equilibrated excited state—influences the steady state emission spectrum and causes time-dependent emission spectra. Although more complex to interpret, environmental and thermal effects in emission spectroscopy carry, in principle, much information on the overall equilibrium and dynamic solvation interactions. In liquid mixtures, the solvent with better solvation properties toward the probe can, in turn, be different for the two states involved in the transition. Changes in preferential solvation between ground and excited states are dynamically controlled by diffusion, adding a time-dependent contribution to the emission spectroscopy.[32,35−37]

In mixtures of solvents of different polarities, preferential solvation (dielectric enrichment) is not only captured by solvatochromism but also by its temperature variation, called thermochromism,[32,38] whose magnitude depends on the sensitivity of the environment around the chromophore when temperature changes.[39,40]

In the present work we studied the local solvent composition inhomogeneities around molecular probes dissolved in two solvent mixtures: water + 2,6-dimethylpyridine (lutidine) and water + pyridine. At atmospheric pressure, the former mixture has a lower critical point at lutidine mass fraction $f_L^c \approx 0.29$ and $T_c \approx 307$ K,[41] whereas the latter mixture does not show liquid−liquid

phase separation. Local concentration inhomogeneities were determined by measuring the solvatochromic shifts of Reichardt's Dye (RD, absorption) and Nile Red (NR, emission), two sensitive solvatochromic compounds (see Scheme 1).

RD is a very well-known solvatochromic probe; its intramolecular charge-transfer absorption energy depends strongly on the polarity of its solvation shell due to the unequal differential solvation of its highly dipolar equilibrium ground state and its less dipolar first Franck−Condon excited state ($\Delta\mu \approx -9$ D) with increasing solvent polarity.[33] In addition, this dye can hydrogen-bond to protic solvents such as alcohols, phenols, and water.[42]

NR is an oxazone probe that has been extensively used to monitor hydrophobic−hydrophilic interactions in biological systems[43] and polarity in synthetic polymers[44] and solvents. The emissive excited state of NR displays an increase of 11 D in the dipole moment with respect to the ground state. This confers a great sensitivity of the emission energy to environment polarity[45,46] while the carbonyl moiety provides sensitivity to the H-bond donation ability of the medium.[46,47]

EXPERIMENTAL DETAILS AND DATA ANALYSIS

Lutidine (2,6-dimethylpyridine, Merck PA) and pyridine (Merck PA) were distilled under vacuum prior to use. Milli-Q deionized water had a conductivity less than 0.1 μS. RD (4-(2,4,6-triphenyl-l-pyridinio)-2,6-diphenylphenolate, Aldrich) and NR (9-(diethylamino)-5H-benzo-[a]phenoxazin-5-one, Aldrich) were used without further purification.

Aqueous mixtures of compositions 0.1 to 1.0 mass fraction of either lutidine or pyridine were prepared by weight (uncertainty $<1 \times 10^{-4}$). Due to the low solubility of RD and NR in water, solutions with mass fraction of organic compound smaller than 0.1 were not studied. RD concentrations were adjusted to keep the absorbance at the maximum wavelength around 0.1. Concentration of NR in the solvent mixture was in the micromolar range.

Absorption spectra were measured in a Varian Cary 50 UV−vis spectrophotometer with a Peltier-thermostatted cell holder (stability ±0.1 K) and appropriate stirring control. Temperature was measured to 0.05 K by means of a thermistor dipped in the solution.

Steady-state excitation and emission spectra were recorded in a PTI QuantaMaster spectrofluorometer. Emission spectra were measured at different excitation wavelengths, from 530 to 580 nm. No red-edge effect was observed. All spectra were corrected by instrumental sensitivity. Spectra with excitation wavelength 560 nm were chosen for the analysis, as they show high fluorescence intensity (large signal-to-noise ratio) and a complete emission spectrum in the accessible wavelength range. Temperature was regulated with a water-circulating thermostat and measured by a thermistor dipped in the solution. The temperature homogeneity along the quartz cuvette was verified near the consolute point by checking the turbidity profile. Fluorescence measurements of NR in pyridine−water (PW) solutions were performed only at 298 K.

Values of the wavenumber at the absorption and emission maxima, ν_{max}, were obtained by adjusting a Gaussian function to the data, for data points with intensities $I > 0.85\ I_{max}$. The uncertainty in ν_{max} is ca. 0.2%.

For each mixture, data were obtained at different temperatures until reaching, visually, phase separation. The position of the meniscus was taken as an indication of the proximity of the critical composition, corresponding to lutidine mass fraction $f_L^c \approx 0.29$.

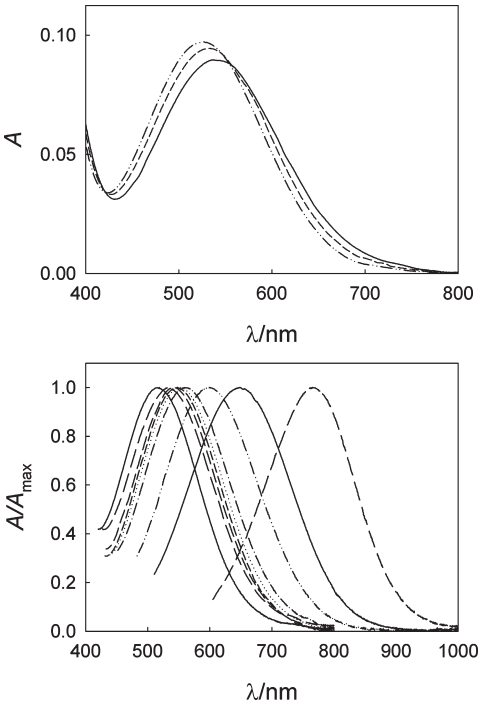

Figure 1. Absorption spectra of RD in LW mixtures for (a) $f_L = 0.2970$ and temperatures of −303, - - 293, and −·· ·−283 K; (b) $T = 305$ K and f_L (from left to right) 0.0994, 0.2008, 0.2970, 0.3982, 0.4921, 0.6025, 0.8018, 0.9036, 1.

The lower critical temperature of the lutidine−water (LW) system ($T_c = 307.1$ K ± 0.2 K) was determined for the critical mixture as the average between the highest temperature without phase separation and the lowest temperature with two liquid phases.

RESULTS

Absorption of RD. Figure 1 shows the absorption spectra of RD dissolved in LW mixtures. Panel a illustrates the thermochromism displayed by a mixture with composition near the critical value at three selected temperatures (303, 293, and 283 K). As shown in the figure, with increase in temperature, the absorption band moves to higher wavelength (red shift). In panel b, the solvatochromic effect is illustrated by showing the spectra at 305 K for mixtures with f_L ranging from 0.1 to 1.0. As the ground electronic state of RD has a larger dipole moment than the excited state, the increase in the concentration of lutidine—a nonpolar substance—decreases the energy of the transition to the excited state, i.e., the addition of lutidine produces a bathochromic shift.

The absorption spectra of RD in the two aqueous mixtures, LW and PW, were measured by Dimroth and Reichardt at 298 K.[48] Figure 2 displays their values of λ_{max}, the maximum absorption wavelength, as a function of the composition of the liquid mixture together with our results. As shown in the figure, our PW data are in good agreement with theirs, except for pure pyridine, where our value is ca. 15 nm lower than previously reported.[48] The difference is most probably due to water absorption, a very frequent contaminant in nonaqueous solvents. Despite being significant, the shift corresponds to a moderate water concentration (mass fraction *ca.* 5×10^{-3}) as in this composition range the position of the absorption maximum is

very sensitive to the water content. Although solvents were distilled before use, atmospheric moisture contamination was difficult to avoid. Actually, we did not make special efforts to circumvent this inconvenience; we just ensured that while changing temperature, the composition of samples remained unaltered. For this reason, during the measurements the samples were contained in spectrophotometer cells with a polytetrafluoroethylene (PTFE) stopper in a ground-type joint, which provided a tight seal for several hours, each sample was measured within a day, and for selected samples (pure pyridine and the sample with near critical LW composition), the spectra at the first measured temperature was checked at the end of the run, to verify the reproducibility of the measurements and the integrity of the sample. Additionally, the composition range of interest in this work is quite far from the pure pyridine or lutidine regions.

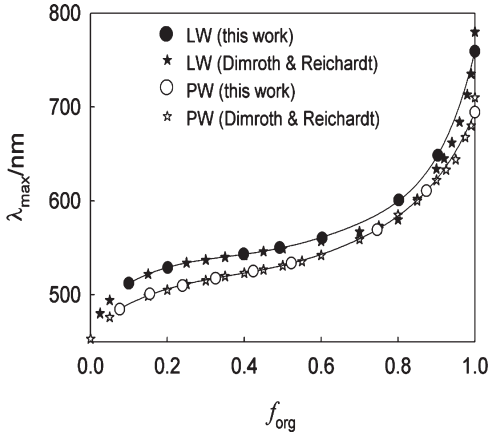

Figure 2. Wavelength of maximum absorption of RD in LW and PW at 298 K as a function of the mass fraction of the organic component. Comparison of data from ref 48 and this work. Lines are only guides for the eye for the present data.

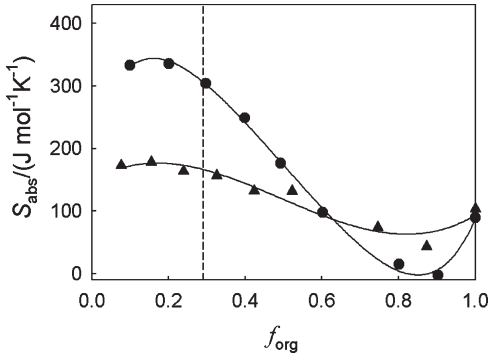

Figure 3. Thermochromic absorption coefficient S_{abs} (defined by eq 1) of RD dissolved in LW (circles) and in PW (triangles), as a function of the mass fraction of the organic component. The vertical dashed line indicates the critical composition of the LW system.

The agreement between our data and Dimroth and Reichardt's for LW mixtures at 298 K is less satisfactory, as depicted in Figure 2. Besides the discrepancy shown at $f_L = 1$, of the same magnitude and possibly having the same origin as observed for pure pyridine, the literature data show a peculiar behavior for lutidine mass fractions around 0.8, where λ_{max} of RD in LW becomes even smaller than those in PW. We have carefully checked our samples but could not reproduce the literature trend in this composition range. Overall, Figure 2 shows that, according to our measurements, the two aqueous systems display similar behavior, the curve for RD in the LW mixture being slightly displaced to higher wavelengths.

All values of λ_{max} were converted to wavenumber, $\nu_{max} = (\lambda_{max})^{-1}$, which is proportional to the transition energy. Its temperature derivative, the thermochromic coefficient S_{abs} of the dye,[38] was calculated for LW and PW mixtures according to

$$S_{abs} = -N_A hc(\partial \nu_{max}/\partial T)_{x,p} \quad (1)$$

where h, c, and N_A denote the Planck's constant, the speed of light, and Avogadro's number, respectively. For RD in both solvent mixtures at all compositions, linear relationships between ν_{max} and T with a negative slope were obtained. This indicates a positive and constant thermochromic coefficient in the temperature range studied (283−305 K) for each solvent upon light absorption. For LW in the range around the critical concentration, the variation is twice as large as that of PW, as depicted in Figure 3. The parameters describing this linear relation between ν_{max} and T are given in Table 1, where the mole fractions of the organic liquids are also reported.

Using the results of the fits, values of ν_{max} at constant temperature were interpolated. Figure 4 depicts the dependence of ν_{max} with the bulk composition of the liquid mixture, either mass fraction f or mole fraction x of the organic liquid, along the two limiting isotherms of this study (283 and 305 K). As can be seen in Figure 4, ν_{max} is not a linear function of either the mass fraction (close to the volume fraction, as densities of the three liquids are near 1 g/cm^3) or the mole fraction. Therefore, our

Table 1. Parameters for the Fit of $\nu_{max} = \nu^*_{max} + (\partial \nu_{max}/\partial T)\,(T - 298\ \mathrm{K})$ to the Absorbance Data of RD in LW and PW Mixtures

LW				PW			
f_L	x_L	$10^{-3}\nu^*_{max}$ (cm^{-1})	$\partial\nu_{max}/\partial T$ (cm^{-1}/K)	f_P	x_P	$10^{-3}\,\nu^*_{max}$ (cm^{-1})	$\partial\nu_{max}/\partial T$ (cm^{-1}/K)
0.0994	0.01822	19.53	−27.8	0.0760	0.01839	20.63	−14.4
0.2008	0.04053	18.91	−28.1	0.1543	0.03990	19.96	−14.9
0.2970	0.06632	18.63	−25.4	0.2393	0.06686	19.62	−13.7
0.3982	0.1001	18.42	−20.8	0.3254	0.09898	19.32	−13.1
0.4921	0.1401	18.21	−14.7	0.4234	0.1433	19.05	−11.1
0.6025	0.2031	17.87	−8.16	0.5226	0.1996	18.72	−11.0
0.8018	0.4048	16.70	−1.27	0.7455	0.4002	17.60	−6.18
0.9036	0.6118	15.42	0. 203	0.8738	0.6119	16.39	−3.59
1	1	13.09	−7.49	1	1	14.34	−8.68

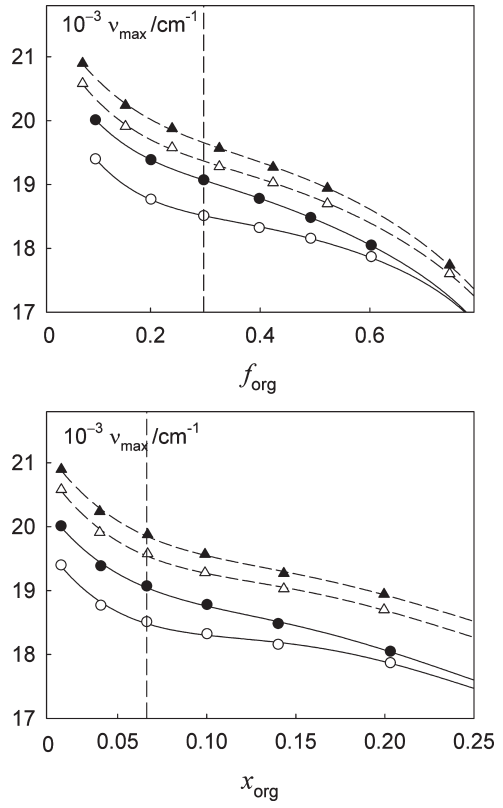

Figure 4. Maximum absorption wavenumber of RD in LW (circles) and PW (triangles) mixtures at 283 K (filled symbols) and 305 K (open symbols) as a function of the composition, given in mass fraction (a) and mole fraction (b). Only the region around the critical composition of the LW mixture (indicated by the vertical dashed line) is shown.

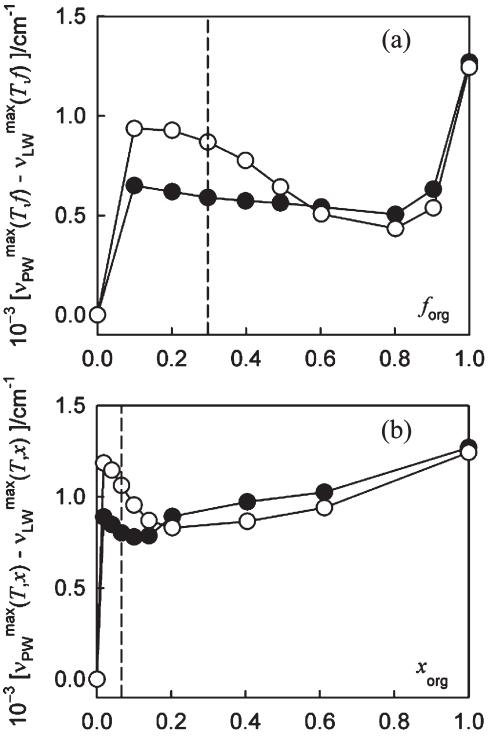

Figure 5. Difference between the maximum absorption wavenumber of RD dissolved in PW and in LW of concentration c (a: mass fraction; b: mole fraction) at two temperature conditions: close to (305 K, open circles) and far from (283 K, filled circles) the critical temperature.

analysis about local density (composition) enhancements will not be based on the deviation from linear behavior but on the comparison between LW (showing phase separation and criticality) and PW (miscible in all proportions).

In order to compare the local compositions around RD in LW and in PW, the values of ν_{max} for the latter mixture were fitted as a function of the pyridine mass fraction f_P at constant temperature by a polynomial, used as an operative fit. With the interpolated values for ν_{max} in PW, we have calculated the difference between the maximum absorption wavenumber of RD in PW and LW at fixed composition and temperature, $\Delta\nu_{RD} = \nu_{max}^{PW}(T,c) - \nu_{max}^{LW}(T,c)$, where c stands for bulk mass fraction or mole fraction of lutidine or pyridine in the mixtures. In particular, we centered our attention to the values of $\Delta\nu_{RD}$ at both the lowest and the highest measured isotherms: T = 283 K (i.e., 22 K from the critical temperature, reduced distance $\Delta T_r = 1 - T/T_c = 0.08$) and T = 305 K (2 K from the critical temperature, $\Delta T_r = 0.007$). Since pyridine has a ν_{max} larger than lutidine, the values of $\Delta\nu$ in the two composition extremes are $\Delta\nu(T,0) = 0$ for pure water (not measured) and $\Delta\nu(T,1) > 0$ for pure pyridine/lutidine [$\Delta\nu(283\text{ K},1) = 1.4 \times 10^3\text{ cm}^{-1}$ and $\Delta\nu(305\text{ K},1) = 1.3 \times 10^3\text{ cm}^{-1}$]. For intermediate compositions, a *monotonous* variation of $\Delta\nu$ between these limits should be observed if the preferential solvation for water of RD in PW and in LW of the same composition are alike. Instead, Figure 5 shows that $\Delta\nu$ presents a maximum for concentrations f_{org} between 0.1 and 0.2, i.e., for values close, but below, the critical concentration of lutidine in LW. Moreover, Figure 5 shows that the maximum is significantly larger for $\Delta\nu$(305 K) than for $\Delta\nu$(283 K), i.e., for temperatures closer to T_c. This result is independent of the concentration scale adopted and is well beyond the uncertainty introduced by the fitting procedure (estimated in 70 cm^{-1}). Taking into account that ν_{max} decreases with the decrease in water concentration (see Figure 4), the positive deviation in $\Delta\nu$ reflects a decrease in the water content of the solvation shell of RD in LW compared to that in PW.

The conclusion from Figure 5 is that, close to the critical concentration, the solvent environment around RD in LW is richer in the organic liquid than expected from its behavior in PW solutions, and that the difference increases as the critical temperature is approached. At first sight, this is an odd result, as the ground state of RD is polar and therefore expected to show more affinity toward water. The interpretation of this experimental evidence is discussed below in detail.

Emission Measurements. Emission spectra of NR in nine solutions of different lutidine concentration were measured at various temperatures. In all cases, a blue shift was observed while increasing temperature at constant composition or lutidine concentration at constant temperature (see Figure 6).

At constant composition, the wavenumber at the maximum ν_{max} can be represented as a linear function of the temperature within the experimental uncertainty. The thermochromic coefficient for the emission (S_{em}) of NR in LW was calculated for the different solutions through the temperature derivative of ν_{max}

$$S_{em} = hcN_A(\partial\nu_{max}/\partial T)_{x,p} \quad (2)$$

The dependence of S_{em} with the composition of the liquid mixture is shown in Figure 7. The positive values of S_{em} for

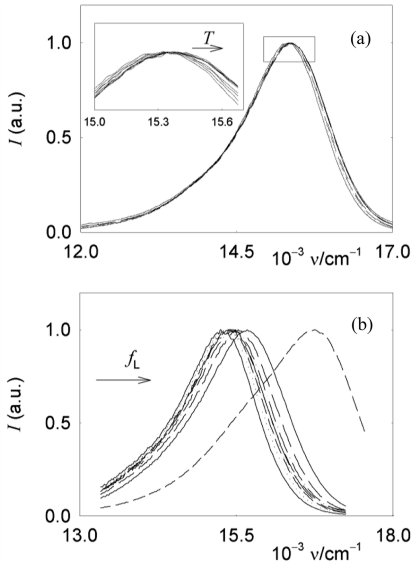

Figure 6. Emission spectra of NR in LW; (a) thermochromic shifts for the f_L = 0.29 solution between 283 and 302 K (from left to right); (b) solvatochromic shift at 298 K for f_L: 0.0992, 0.1970, 0.2901, 0.4054, 0.5004, 0.6039, 0.7002, 0.8003, and 1 (left to right).

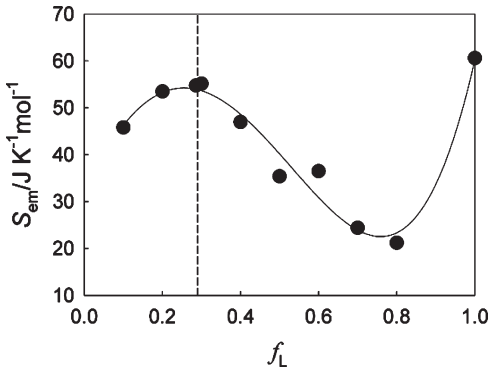

Figure 7. Thermochromic emission coefficient S_{em} (defined by eq 2) of NR dissolved in LW solutions as a function of the lutidine mass fraction. The vertical dashed line indicates the critical composition while the solid line is a guide for the eyes.

NR can be interpreted as a stronger interaction of the probe with the medium in the excited state than in the ground state.[49]

Interestingly, despite referring to different probes, the shape of the emission (Figure 7) and absorption (Figure 3) thermochromic coefficients for LW are quite similar, and both point to an anomalous increase in the thermochromic effect near the critical composition.

Figure 8 depicts the dependence of ν_{max} with the concentration (a: mass fraction; b: mole fraction) for NR in LW at 283 and 306 K (i.e., at ca. 24 and 1 K from the critical temperature of the mixture) and for PW at 298 K.

From Figure 8, it can be concluded that PW shows a smooth dependence of ν_{max} with concentration, especially on x (mole fraction) more than on f (mass fraction). By contrast, the values obtained for LW mixtures show, in both representations, a change in curvature at concentrations near the critical concentration (see insets in Figure 8), and that anomaly is more pronounced the closer to the critical isotherm (307 K).

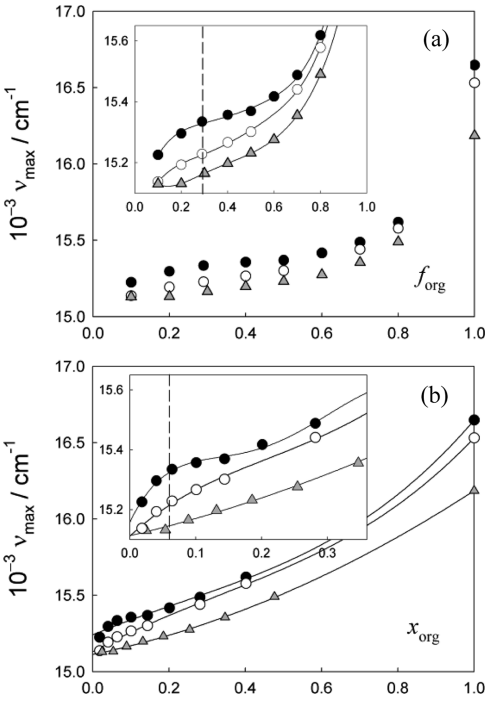

Figure 8. Emission wavenumber maxima (ν_{max}) of NR in LW (circles) and PW (triangles) as a function of the concentration: (a) mass fraction, (b) mole fraction. For LW data, temperatures are 306 (black) and 283 (white) K while for the PW system, T = 298 K.

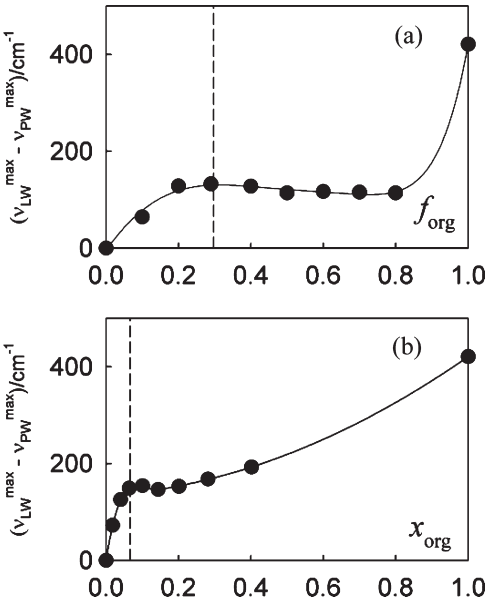

Figure 9. Difference between the emission wavenumber of NR dissolved in solutions of LW and PW of equal concentration at 298 K, as a function of the concentration of the organic component: (a) mass fraction, (b) mole fraction.

The difference in the position of the emission maximum of NR between LW (ν_{max}^{LW}) and PW (ν_{max}^{PW}) solutions at 298 K and at constant composition was calculated in a fashion similar to that for the absorption measurements. In this case, the $\Delta\nu_{NR}$ is defined as $\Delta\nu_{NR} = \nu_{max}^{LW}(298\ K,c) - \nu_{max}^{PW}(298\ K,c)$, where again c

stands for the mass or mole fraction of lutidine or pyridine in the mixtures. To obtain the values for particular concentrations in both systems, we proceeded in the same way as explained for RD absorption. The result is depicted in Figure 9a (for $c = f_{org}$) and Figure 9b (for $c = x_{org}$). These results are qualitatively similar to those in Figure 5: at 298 K, $\Delta\nu_{NR}$ is not a monotonous function of the bulk composition.

DISCUSSION

Both the solvatochromism and thermochromism determined in the present study show revealing aspects. The first interesting feature is the similarities between Figures 5 and 9, showing the difference between LW and PW in the composition dependence of the solvatochromism of the dyes. For both RD absorption and NR emission, the solvatochromism in LW mixtures near the critical composition can be interpreted as an increase in the lutidine present in the solvation shell, compared with bulk or with PW mixtures of the same proportion. Figure 5 shows that this notable difference of LW mixtures compared to PW increases as the critical temperature is approached. The second feature arises from the comparison of Figure 3 and 7: for both dyes, there is a maximum in the absolute value of $(\partial\nu_{max}/\partial T)$, i.e., in the thermochromic coefficient of the transition, around the critical concentration in LW mixtures, which is absent in the RD−PW system. We attribute both of these characteristics to the critical phenomenon and point out the sensitivity of the thermochromic component.

RD and NR are both lipophilic dyes that exhibit large shifts in the absorption and emission, respectively, as the solvent polarity is changed, since their ground and excited states differ strongly in their dipole moment.[33,45] NR is poorly soluble in water, and the small amounts dissolved show photochemical properties that were interpreted as being due to aggregation,[46] an indication of the poor overall solvation capacity of pure water for these solutes. Moreover, RD is insoluble in water within the detection limit. On the other hand, both probes exhibit high solubility in pure lutidine or pyridine and a strong dependence of the absorption or emission wavenumber on the addition of small amounts of water.

These observations suggest that most sites of both probe molecules are better solvated by nonpolar solvents, but that the presence of polar H_2O molecules significantly modifies their electronic energies by interacting with specific sites of the probes. A simplified picture of the solvation shell around these molecules should show a predominant amount of nonpolar solvent molecules around the 5 phenyl groups of the RD or around most of the NR (see Scheme 1). However, the groups with higher charge density, such as the pyridinium and phenolate groups of RD or the amino and carbonyl groups of the NR molecules, should specifically interact strongly with water molecules. These differences in the solvation shell are promoted by short-range interactions between moieties with different electronic densities in the probe molecules and this mixture of solvent molecules with different polarities.

As mentioned in the Introduction, the near-critical region is characterized by extended and persistent domains of densities (concentration) different form the average value. The size of these domains, the correlation length ξ, depends on the distance to the critical point. For the particular case of LW, at 24, 9, and 1 K away from T_c, the values of ξ are ca. 1, 2, and 7 nm,[50] respectively. These domains ("nanodroplets" of L-rich or W-rich phases) of increasing size may interfere with the short-range solvation of the probe. Our results show that, as the critical point is approached, the *less polar* solvent component is favored in the solvation shell. Our interpretation is that, since most sites of both probe molecules are solvated by lutidine, critical correlations hamper the proper solvation by water, probably by disturbing the distance or orientation between water molecules and probe. This is evidenced as an anomalous red shift of RD absorption (Figure 4) or a blue shift of NR emission (Figure 8) in LW mixtures around the critical composition as the critical temperature is approached, indicating an increase of lutidine concentration as compared with PW for the same composition range (Figures 5 and 9). From these results, the behavior of LW systems seems to be a consequence of the critical phenomenon.

To support this contention, we highlight the effect of temperature obtained for the present system (with a lower critical point) in comparison with the one normally observed for gas−liquid critical points. In the latter case (for example, anthracene in C_2H_6), the *increase* in temperature, which takes the system away from the critical temperature, leads to a *decrease* in the extent of the observed local augmentation.[16] However, the origin of this diminishing effect was not conclusively established: it could be due to the increase in the distance to the critical point (effect of critical fluctuations) or it could be related to the decrease of the attractive interactions as the temperature increases (Boltzmann factor). In contrast to these results, the peculiar concentration dependence (increase of lutidine concentration around RD or NR, compared to that of pyridine, seen in Figures 5 and 9) of the probe signal in the LW system disappears slowly as the systems moves toward lower temperatures, also away from the critical temperature. Therefore, we discard thermal effects as the origin of our results. It could be argued that also the hydrogen-bond between water and the probe becomes weaker as the temperature increases, and that this effect would also reduce the water concentration around the solvatochromic molecule, but the effect of partial "dehydration" of the probe is not displayed in the PW system, and therefore we do not expect it to be relevant at the temperature range presently studied.

Besides the divergence of the correlation length, diffusional times τ (or fluctuation lifetimes) increase very strongly as the critical point is approached, an effect known as *critical slowing down*. For LW at 24, 9, and 1 K away from T_c, the values of τ are ca. 2, 10, and 2×10^3 ns.[51] Absorption measurements are insensitive to the relaxation of the probe's environment after probe electronic excitation, i.e., solvatochromism of RD reflects the equilibrated composition of the near environment of the probe in the ground state. In contrast, the emission spectra reflect the changes in the solvation shell of the emitting species during the excited-state lifetime (for NR ca. 3 ns).[45,46,52]

After electronic excitation, polarizability effects due to the electrons occur almost instantaneously, affecting both light absorption and emission. On the other hand, the emission occurs after the solvation of the excited state has had an opportunity to relax toward equilibrium. However, there are different time scales involved in the relaxation: reorientation of solvent molecules in the field of the excited probe is relatively fast (of the order of picoseconds), and translational movements (diffusional), which account for the different average solvation shell composition in the ground and in the excited state of the probe, are usually much slower than rotational effects.[34]

According to the values of fluctuation lifetimes mentioned above, only at around 30 K from the critical point (i.e., at ca. 277 K) would the time τ required by the domains to diffuse become on the order of magnitude of the excited state lifetime. However, under

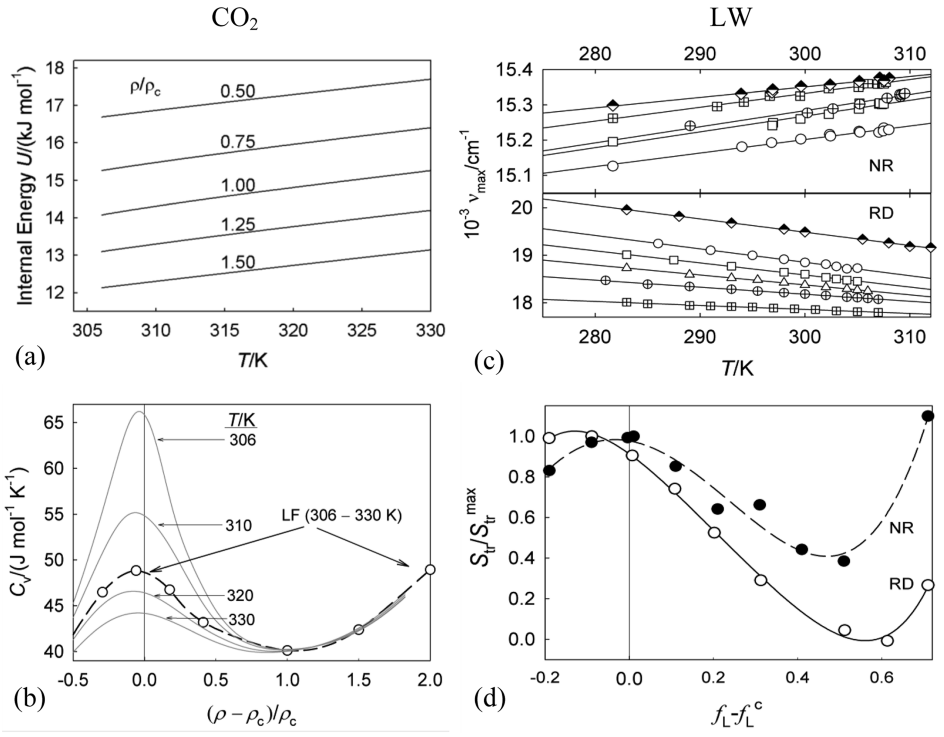

Figure 10. Comparative behavior of a pure fluid (CO_2, (a,b)) and a binary mixture (LW, (c,d)) near their respective critical points. For CO_2, (a) internal energy U along isochors; (b) solid lines: constant volume heat capacity C_v; circles and dashed line: slopes of the isochores in panel a, assuming U as a lineal function of T. For LW, (c) ν_{max} of NR (upper) and RD (lower) along isopleths; (d) thermochromic coefficient S_{tr} for NR and RD reduced by their respective maximum value.

these conditions, the anomalous behavior near the critical composition is very mild or undistinguishable (see Figures 4 and 8, curves at 283 K for LW). Therefore we did not perform time-resolved emission spectroscopy for NR in LW mixtures and consider that the solvatochromic similarities shown by both dyes is a support for the influence of the critical phenomena on the spectroscopic features.

A remarkable result of this work is the sensitivity of thermocromism to point out the presence of critical fluctuations, even at temperatures relatively far from the critical one. Thermochromic singularity is present in both dyes as a maximum in the absolute value of the temperature coefficient of ν_{max} of absorption of RD or emission of NR at roughly the same LW composition. No such singularity is present in the PW mixtures.

To explain the observed thermochromic behavior, we analyzed our results in the context of the critical phenomena, taking advantage of the isomorphism principle, i.e., of the similarities displayed by very different kinds of systems when described in terms of the appropriate thermodynamic variables.

The property studied, the transition (absorption or emission) energy $hc\nu_{tr}$, can be considered as having two contributions: the first is the difference in energy between ground and excited states of the *isolated* probe molecule, $hc\nu_{tr}^{isol}$, while the second includes the solvent-induced contribution to the transition energy ($hc\nu_{tr}^{solv}$):

$$hc\nu_{tr} = hc\nu_{tr}^{isol} + hc\nu_{tr}^{solv}$$
$$N_A hc\nu_{tr}^{solv} = \rho \sum_{i=L,W} x_i \int g_{iM}(r)\Delta\omega_{iM}(r_{iM}) d\vec{r}_{iM} \quad (3)$$

Equation 3 gives an expression for the second contribution, the average solvation energy difference, in terms of $g_{iM}(r)$, the pair correlation function between solvent molecules of type i (W or L) and probe molecule M (either in the ground state, for ν_{abs}, or in the first excited state, for ν_{em}). The function $\Delta\omega_{iM}(r) = (\omega_{iM^*} - \omega_{iM})$ represents the difference in the effective interaction potential of solvent i with the excited (ω_{iM^*}) and the ground (ω_{iM}) states of M; this effective potential $\omega_{iM} = u_{iM} + B_{iM}/2$ includes, in addition to the pair potential u_{iM}, the binding energy of solvent molecules B_{iM}, which takes into account the average interaction energy of a solvent molecule i with the surrounding solvent molecules.[38] Near the critical point, all the g_{iM}'s show the same anomalous features displayed by g_{WW}, g_{LW}, and g_{LL}: a long-range "tail" (decaying approximately as $\exp(-\xi/r)r^{-1}$) and a short-range behavior essentially unaffected by criticality. On the other hand, the pair potentials u_{iM} and u_{iM^*} are short-ranged, as are B_{iM} and B_{iM^*}. Therefore, the value of ν_{tr}^{solv} is expected to be determined by the short-range part of g_{iM}, which, as said, does not display any critical anomaly. More interesting, the expression for ν_{tr}^{solv} given in eq 3 has the same form as that of the residual internal energy of a one-component system

$$U^r = U - U^{id} = \frac{\rho}{2}\int g(r)u(r)\, d\vec{r} \quad (4)$$

indicating that the two properties, ν_{tr}^{solv} and U^r, will behave in a similar way in near-critical conditions. As discussed by Levelt Sengers,[53] "U^r has no conspicuous critical effect, although there are some subtleties" as its temperature derivative, the constant-volume heat capacity C_v, displays a *weak* divergence along the critical isochore: $C_v = At^{-\alpha}$ (with A an amplitude, t the reduced critical temperature, $t = \Delta T/T_c$, and the critical exponent $\alpha = 0.11$). Due to the similarities in eqs 3 and 4, one can anticipate that ν_{tr} should be well-behaved at any concentration (as is U^r at any density),

but that its temperature derivate should display a weak (α-like) anomaly at the critical point of the solvent mixture, as does C_v of a pure fluid.

To illustrate this argument, Figure 10 depicts U and C_v for pure fluid (CO_2, T_c = 304.13 K, ρ_c = 10.625 mol/dm^3) together with ν_{max} and S_{tr} for RD and NR dissolved in LW, in both cases relatively close to their critical points. Figure 10a shows the behavior of the internal energy U for CO_2 in the supercritical regime as a function of the temperature along several isochores, (labeled by their reduced critical density, ρ/ρ_c).[54] The data span the 306−330 K temperature range (2−26 K away from T_c), i.e., they are strictly outside the asymptotic region. As shown in Figure 10a, in this range the isochores can be roughly represented as linear functions of the temperature, although the correct dependence for the critical isochore is $U \propto (T/T_c - 1)^{1-\alpha} = (T/T_c - 1)^{0.89}$. Figure 10c depicts the dependence of ν_{max} of NR (top) and RD (bottom) in the one-phase region as a function of the temperature along several isopleths, (labeled by their lutidine mass fraction f_L) in the 283−305 K range (24−2 K away from T_c), i.e., also outside the asymptotic region. The data show a linear dependence with T at our level of experimental precision and of proximity to the critical point. Figure 10b shows that the values of $C_v = (dU/dT)_V$ for CO_2 along several supercritical isotherms (solid curves) display maxima at $\rho \approx \rho_c$, and the closer the isotherm to T_c, the larger the value of the maximum. The dashed curve and the circles in Figure 10b indicate the slopes of the isochores in Figure 10a, taken as linear function of T. These values are obviously independent of temperature, but they exhibit the same shape as the C_v curves, in particular a maximum at $\rho \approx \rho_c$. Finally, Figure 10d represents S_{tr}, the thermochromic coefficient, obtained assuming a linear dependence of ν_{max} with T, as a function of $(f_L - f_L^c)$. As anticipated above, although the calculated temperature coefficient of ν_{max} does not diverge and is independent of the temperature, it behaves like the temperature coefficient of U data obtained outside the asymptotic region and assuming linear temperature dependence. We therefore attribute the maxima in the thermochromic coefficient observed for both dyes to the critical susceptibility and point out specially its sensitivity.

OVERALL CONCLUSION

The use of a different experimental strategies to establish unambiguously the existence of LDA has been successfully implemented in this work. It should be noted that it is the first time critical enhancements were studied in systems with binary solvents in the neighborhood of a lower liquid−liquid consolute critical point. The solvatochromic effect in the vicinity of a lower consolute point has the advantage that the Boltzmannian temperature dependence of intermolecular interactions (increasing temperature decreases their importance) is opposite to that of the critical enhancement where an increase of temperature, approaching the critical consolute point, enhances the influence of criticality upon the properties of the system.

Moreover, the judicious choice of sensitive attractive probes allowed us to determine unequivocally the characteristics of the local composition around them, compared with the composition of the bulk. The attractive probes dissolved in LW mixtures showed that, as the critical consolute point is being approached, the solvatochromism differs significantly from that observed in PW mixtures; in particular it exhibits a lower local water concentration than for the PW binary solvent. Interestingly, the thermochromism observed for both probes in LW mixtures shows a maximum near the critical concentration, which is absent for the PW system. Hence it indicates clearly that the closeness to the LW critical point is responsible for the enhanced organic solvent (lutidine) concentration, which is not observed for pyridine in the PW system.

AUTHOR INFORMATION

Corresponding Author

*Phone: +54 11 6772 7194; fax: +54 11 6772 7886; e-mail: mljapas@cnea.gov.ar.

ACKNOWLEDGMENT

K.I.G., P.F.A., and R.F.P. are Research Staff from CONICET (Consejo Nacional de Investigaciones Científicas y Técnicas, Argentina). Research was partially supported by Proy. Inv. Prg22-Pry05-Obr51 and grants X-006 (UBA) and PICT 33973 and 14332 (ANPCyT) of Argentina.

REFERENCES

(1) For a number of reviews covering both fundamental aspects and applications in SCFs, see *Chem. Rev.* **1999**, *99*, issue 2.
(2) Kajimoto, O. *Chem. Rev.* **1999**, *99*, 355–389.
(3) Song, W.; Biswas, R.; Maroncelli, M. *J. Phys. Chem. A* **2000**, *104*, 6924–6939.
(4) Brennecke, J. F.; Chateauneuf, J. E. *Chem. Rev.* **1999**, *99*, 433–452.
(5) Sciaini, G.; Marceca, E.; Fernández-Prini, R. *Phys. Chem. Chem. Phys.* **2002**, *4*, 3400–3406.
(6) Fernández-Prini, R. *J. Phys. Chem. B* **2002**, *106*, 3217–3225.
(7) Egorov, S. A. *J. Chem. Phys.* **2000**, *113*, 1950. Egorov, S. A. *J. Chem. Phys.* **2000**, *112*, 7138–7146. Egorov, S. A. *J. Chem. Phys.* **2002**, *116*, 2004–2010.
(8) Tucker, S. C. *Chem. Rev.* **1999**, *99*, 391–418. Goodyear, G.; Maddox, M. W.; Tucker, S. C. *J. Chem. Phys.* **2000**, *112*, 10327–10339. Maddox, M. W.; Goodyear, G.; Tucker, S. C. *J. Phys. Chem. B* **2000**, *104*, 6240–6247. Maddox, M. W.; Goodyear, G.; Tucker, S. C. *J. Phys. Chem. B* **2000**, *104*, 6266–6270.
(9) Su, Z.; Maroncelli, M. *J. Chem. Phys.* **2006**, *124*, 164506.
(10) Johnston, K. P.; Haynes, C. *AIChE J.* **1987**, *33*, 2017. Kim, S.; Johnston, K. P. *Ind. Eng. Chem. Res.* **1987**, *26*, 1206. Ikushima, Y.; Saito, N. *J. Phys. Chem.* **1992**, *96*, 2293. Zhang, J.; Roek, D. P.; Chateauneuf, J. E.; Brennecke, J. F. *J. Am. Chem. Soc.* **1997**, *119*, 9980. Schwarzer, S.; Troe, J.; Zerezke, M. *J. Chem. Phys.* **1997**, *107*, 8380.
(11) Chen, J.; Shen, D.; Wu, W.; Han, B.; Wang, B.; Sun, D. *J. Chem. Phys.* **2005**, *122*, 204508.
(12) Oka, H; Kajimoto, O. *Phys. Chem. Chem. Phys.* **2003**, *5* 2535–2540.
(13) Urdahl, R. S.; Myers, D. J.; Rector, K. D.; Davis, P.H..; Cherayil, B. J.; Fayer, M. D. *J. Chem. Phys.* **1997**, *107*, 3747. **1996**, *105*, 8973.
(14) Cabaço, M. I.; Besnard, M.; Tassaing, T.; Danten, Y. *Pure Appl. Chem.* **2004**, *76*, 141–146. Lalanne, P.; Tassaing, T.; Danten, Y.; Cansell, F.; Tucker, S. C.; Besnard *J. Phys. Chem. A* **2004**, *108*, 2617–2624. M. Cabaço, M. I.; Longelin, S.; Danten, Y.; Besnard, M. *J. Phys. Chem. A* **2007**, *111*, 12966–12971.
(15) Heitz, M. P.; Maroncelli, M. *J. Phys. Chem. A* **1997**, *101*, 5852.
(16) Lewis, L. E.; Biswas, R.; Robinson, A. G.; Maroncelli, M. *J. Phys. Chem. B* **2001**, *105*, 3306.
(17) Sun, Y. P.; Fox, M. A.; Johnston, K. P. *J. Am. Chem. Soc.* **1992**, *114*, 1187.
(18) Betts, T. A.; Zagrobelny, J.; Bright, F. V. *J. Am. Chem. Soc.* **1992**, *114*, 8163.
(19) Randolph, T. W.; Carlier, C. *J. Phys. Chem.* **1992**, *96*, 5146–5151.
(20) O'Shea, K. E.; Combes, J. R.; Fox, M. A.; Johnston, J. P. *Photochem. Photobiol.* **1991**, *54*, 571–576. Tanko, J. M.; Pacut

R. *J. Am. Chem. Soc.* **2001**, *123*, 5703–5709. Hoijemberg, P. A.; Zerbs, J.; Japas, M. L.; Chesta, C. A.; Schroeder, J.; Aramendía, P. F. *J. Phys. Chem. A* **2009**, *113*, 5289–5295.

(21) Howdle, S. M; Bagratashvili, V. N. *Chem. Phys. Lett.* **1993**, *214*, 215–219.

(22) deGrazia, J. L.; Randolph, T. W.; O'Brien, J. A. *J. Phys. Chem. A* **1998**, *102*, 1674–1681.

(23) Schwarzer, S.; Troe, J.; Votsmeier, M.; Zerezke, M. *J. Chem. Phys.* **1996**, *105*, 3121. Benzlerm, J.; Linkersdorfer, J.; Luther, K. *J. Chem. Phys.* **1997**, *106*, 4992. Lee, M.; Hotom, G. R.; Hochstrasser, R. M. *Chem. Phys. Lett.* **1985**, *118*, 359.

(24) Myers, D. J.; Shigeiwa, M.; Fayer, M. D.; Cherayi, B. J. *J. Phys. Chem. B* **2000**, *104*, 2402–2414.

(25) Levelt Sengers, J. M. H. *Fluid Phase Equilib.* **1986**, *30*, 31–39.

(26) Anisimov, M. A. *Critical Phenomena in Liquids and Liquid Crystals*; Gordon and Breach Science Publishers: New York, 1991.

(27) Levelt Sengers, J. M. H.; Given, J. A. *Mol. Phys.* **1993**, *80*, 899.

(28) Buback, M.; Franck, E. U. *Ber. Bunsen-Ges. Phys. Chem.* **1972**, *76*, 350.

(29) McRae, E. G. *J. Phys. Chem.* **1957**, *61*, 562–572.

(30) Lakowicz, J. R. *Principles of Fluorescence Spectroscopy*, 2nd ed.; Kluwer Academic Plenum Publishers: New York, 1999; Chapter 6, p 187.

(31) Braslavsky, S. E. *Pure Appl. Chem.* **2007**, *79*, 293–465.

(32) Suppan, P. *J. Chem. Soc., Faraday. Trans. 1* **1987**, *83*, 495.

(33) Reichert, C. *Chem. Rev.* **1994**, *94*, 2319–2358.

(34) Marini, A.; Muñoz-Losa, A.; Biancardi, A.; Mennucci, B. *J. Phys. Chem. B* **2010**, *114*, 17128–17135.

(35) Betts, T. A.; Bright, F. V. *Appl. Spectrosc.* **1990**, *44*, 1203.

(36) Wetzler, D. E.; Chesta, C.; Fernández-Prini, R.; Aramendía, P. F. *J. Phys. Chem. A* **2002**, *106*, 2390–2400.

(37) Turro, N. J. *Modern Molecular Photochemistry*; University Science Books: Sausalito, CA, 1991.

(38) Matyushov, D. V.; Schmid, R.; Ladanyi, B. M. *J. Phys. Chem. B* **1997**, *101*, 1035–1050.

(39) Kavarnos, G. J.; Turro, N. J. *Chem. Rev.* **1986**, *86*, 401–449.

(40) Wetzler, D. E.; Fernández-Prini, R. J.; Aramendía, P. F. *Chem. Phys.* **2004**, *305*, 27–36.

(41) Kaatze, U.; Woermann, D. *J. Phys. Chem.* **1984**, *88*, 284–288.

(42) Coleman, C. A.; Murray, C. J. *J. Org. Chem.* **1992**, *57*, 3578–3582.

(43) Klymchenko, A. S.; Duportail, G.; Demchenko, A. P.; Mély, Y. *Biophys. J.* **2004**, *86*, 2929–2941.

(44) Hou, Y.; Bardo, A. M.; Martinez, C.; Higgins, D. A. *J. Phys. Chem. B* **2000**, *104*, 212–219.

(45) Dutt, G. B.; Doraiswamy, S.; Peryasami, N.; Venkataraman, B. *J. Chem. Phys.* **1990**, *82*, 8498.

(46) Dutta, A. K.; Kamada, K.; Ohta, K. *J. Photochem. Photobiol. A: Chem.* **1996**, *93*, 57–64.

(47) Gonheim, N. *Spectrochim. Acta, A* **2000**, *56*, 1003–1010.

(48) Dimroth, K.; Reichardt, C. *Z. Anal. Chem.* **1966**, *215*, 344–350.

(49) Boldrini, B.; Cavalli, E.; Painelli, A.; Terenziani, F. *J. Phys. Chem. A* **2002**, *106*, 6286–6294.

(50) Gülari, E.; Collings, A. F.; Schmidt, R. L.; Pings, C. J. *J. Chem. Phys.* **1972**, *56*, 6169.

(51) Diffusional times τ were calculated assuming $\tau = 6\pi\eta\xi^3/k_BT$.

(52) Cser, A.; Nagy, K.; Biczók, L *Chem. Phys. Lett.* **2002**, *360*, 473–478.

(53) Levelt Sengers, J. M. H. In *Supercritical Fluids Technology*; Bruno, T. J., Ely, J. F., Eds.; CRC Press: Boca Raton, FL, 1991.

(54) Lemmon, E. W.; McLinden, M. O.; Huber, M. L. *REFPROP, Reference Fluid. Thermodynamic and Transport Properties Database 23*, version 8.0; NIST: Gaithersburg, MA, 2007.